Article

Current Biology

Environmental Geometry Aligns the Hippocampal Map during Spatial Reorientation

Highlights

- Environmental shape determined hippocampal map alignment after disorientation
- Nongeometric cues did not resolve geometric ambiguities in map alignment
- Hippocampal map alignment predicted goal-oriented navigational behavior

Authors

Alex T. Keinath, Joshua B. Julian, Russell A. Epstein, Isabel A. Muzzio

Correspondence

isabel.muzzio@utsa.edu

In Brief

The mechanisms underlying spatial reorientation have been at the heart of numerous debates about the nature of cognition. Here, Keinath et al. show that after disorientation, the hippocampal map aligns to the shape of local space and predicts navigational behavior. This suggests that reorientation involves geometric alignment of a cognitive map.

Keinath et al., 2017, Current Biology *27*, 309–317
February 6, 2017
http://dx.doi.org/10.1016/j.cub.2016.11.046

CellPress

Current Biology
Article

Environmental Geometry Aligns the Hippocampal Map during Spatial Reorientation

Alex T. Keinath,[1] Joshua B. Julian,[1] Russell A. Epstein,[1] and Isabel A. Muzzio[2,3,*]
[1]Department of Psychology, University of Pennsylvania, 3710 Hamilton Walk, Philadelphia, PA 19104, USA
[2]Department of Biology, University of Texas at San Antonio, 1 UTSA Circle, San Antonio, TX 78249, USA
[3]Lead Contact
*Correspondence: isabel.muzzio@utsa.edu
http://dx.doi.org/10.1016/j.cub.2016.11.046

SUMMARY

When a navigator's internal sense of direction is disrupted, she must rely on external cues to regain her bearings, a process termed spatial reorientation. Extensive research has demonstrated that the geometric shape of the environment exerts powerful control over reorientation behavior, but the neural and cognitive mechanisms underlying this phenomenon are not well understood. Whereas some theories claim that geometry controls behavior through an allocentric mechanism potentially tied to the hippocampus, others postulate that disoriented navigators reach their goals by using an egocentric view-matching strategy. To resolve this debate, we characterized hippocampal representations during reorientation. We first recorded from CA1 cells as disoriented mice foraged in chambers of various shapes. We found that the alignment of the recovered hippocampal map was determined by the geometry of the chamber, but not by nongeometric cues, even when these cues could be used to disambiguate geometric ambiguities. We then recorded hippocampal activity as disoriented mice performed a classical goal-directed spatial memory task in a rectangular chamber. Again, we found that the recovered hippocampal map aligned solely to the chamber geometry. Critically, we also found a strong correspondence between the hippocampal map alignment and the animal's behavior, making it possible to predict the search location of the animal from neural responses on a trial-by-trial basis. Together, these results demonstrate that spatial reorientation involves the alignment of the hippocampal map to local geometry. We hypothesize that geometry may be an especially salient cue for reorientation because it is an inherently stable aspect of the environment.

INTRODUCTION

A map, cognitive or otherwise, can be a very useful tool for navigation. It can help a navigator find goals, remember where things are located, and plan novel routes. Yet a map is only effective if the navigator understands where she is on the map and which direction she is facing. Under normal navigating conditions, these internal representations of position and heading can be updated based on self-generated (idiothetic) cues, a process known as path integration [1]. However, on occasion, even the best navigator will become disoriented, in which case their estimates of position and heading will be inaccurate. The navigator must then rely on external (allothetic) cues to regain their bearings—a process known as spatial reorientation.

An extensive behavioral literature suggests that the shape of the local navigable space—the *spatial geometry* of the environment—is an especially powerful cue for reorientation [2, 3]. In a now-classic paradigm [4], a disoriented navigator is trained to locate a reward in a corner of a small rectangular chamber. By observing where the navigator subsequently searches for the reward, the cues guiding reorientation can be inferred. Results indicate that navigators search not only at the correct corner but also the diagonally opposite corner, which is a geometrically equivalent location [4]. Thus, navigators behave as if guided by the spatial geometry of the chamber. Notably, nongeometric cues that could potentially distinguish the geometrically equivalent corners, such as a marking along one wall, are often ignored. This pattern of results—observed across numerous species, including birds [5], rodents [4, 6], and humans [7]—indicates that reorientation behavior is strongly informed by the spatial geometry of the environment.

These behavioral results are important because they speak to the cognitive mechanisms mediating reorientation [2, 3, 8–13]. Although any landmark could in theory be used to determine one's heading after disorientation, the strong reliance on geometry suggests that the behavior of the animal is driven by a mechanism that uses global shape parameters of the environment to realign the navigator's cognitive map [4, 14, 15]. This view remains controversial, however, in part because these results can be alternatively explained without any reference to a cognitive map. Under this competing theory, navigation following disorientation is controlled by an egocentric strategy in which goals are reached by moving to a point where the current visual input matches a stored representation of the visual input at the goal location [16–18]. In this view, "reorientation" primarily involves visual recognition, not the recovery of spatial representations.

Adjudicating between these theories on the basis of behavioral data alone has been difficult, but neural data offer a possible

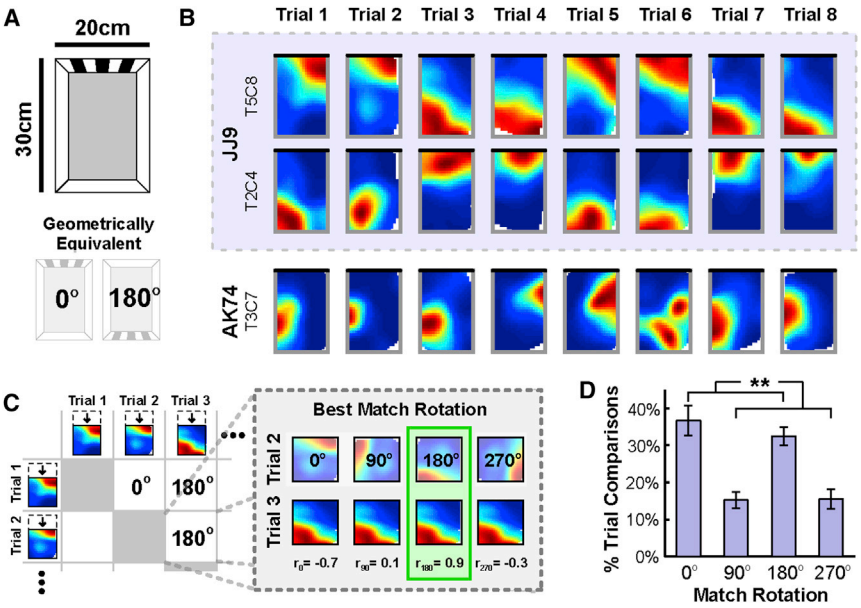

Figure 1. Spatial Geometry Orients a Reliable Hippocampal Map following Disorientation in a Rectangular Chamber

(A) Schematic of the rectangular chamber and the polarizing visual cue. Note that two rotations of this chamber, 0° and 180°, result in geometrically equivalent shapes.

(B) Example rate maps from the first eight trials for three place cells, two of which were simultaneously recorded (blue shading). Black line indicates the location of the visual cue.

(C) Quantification of best-match rotations. To quantify the orientation of rate maps across trials for each place cell, the rotation that yielded the best match (highest correlation) between the two rate maps for each pair of trials was determined.

(D) Distribution of best-match rotations across animals, computed as the percent of pairwise trial comparisons for which each rotation yielded the best match. The 0° and 180° rotations most often and equally often yielded the best match, mirroring the rotational symmetry of the rectangular chamber. All error bars denote ±1 SEM across animals. See also Figure S1. $^{**}p < 0.01$.

opportunity. Lesion, electrophysiology, and functional neuroimaging studies have demonstrated that allocentric and egocentric navigational strategies are mediated by different neuroanatomical structures. Specifically, allocentric strategies are supported by a neural circuit that includes the hippocampus and neighboring structures, whereas egocentric strategies are mediated by extra-hippocampal circuits [19–24]. Therefore, to test whether an allocentric mechanism mediates spatial reorientation, we set out to characterize the hippocampal representations of mice during this process.

Surprisingly, although there is an abundance of research examining hippocampal representations in oriented animals, little is known about how these representations are affected by disorientation. Principal cells in the hippocampus, known as place cells, become active when the navigator occupies a particular location within the environment [21, 25]. These location-specific firing fields form a ''hippocampal map'' that is unique to the navigational context [26]. The hippocampus receives converging inputs from multiple sources and functional cell types [27, 28], and under oriented conditions, a mixture of geometric, nongeometric, and idiothetic cues combine to support a reliable, oriented hippocampal map [29–31]. However, the nature of this map following disorientation is less clear. Previous studies examining place cell responses in chambers containing nongeometric cues but without orienting geometry have yielded conflicting results, with some findings suggesting that the hippocampal map is unstable following disorientation [32] and others suggesting that this map is stable and can be oriented by nongeometric cues [33]. Related work examining head direction (HD) cells, whose activity correlates with the alignment of the hippocampal map under oriented conditions, has yielded similar discrepancies in disoriented animals [32, 34–37], though some studies suggest a privileged role for spatial geometry [38, 39]. Thus, whether the hippocampal map is oriented by geometry following disorientation and whether this map relates to reorientation behavior remain unresolved.

If spatial reorientation relies on a mechanism whereby the cognitive map is recovered relative to global shape parameters, then both the hippocampal map and reorientation behavior should be similarly oriented by spatial geometry. If instead spatial reorientation is mediated by an egocentric view-matching mechanism, then the hippocampal map might be unreliable after disorientation or consistently oriented by prominent visual features, with no predictive relationship between the hippocampal map and reorientation behavior. To test these hypotheses, we recorded place cells as disoriented mice repeatedly explored three chambers, each of a different shape and containing an additional distinct visual cue specifying a unique direction within the chamber. We then recorded hippocampal activity as disoriented mice completed the classic spatial reorientation paradigm in a rectangular chamber. To anticipate, we found that a reliable hippocampal map was recovered across trials and that the spatial geometry alone consistently oriented this map; moreover, the orientation of the hippocampal map predicted reorientation behavior on a trial-by-trial basis. Together, these results highlight the role of spatial geometry as a critical cue orienting the hippocampal map and strongly implicate allocentric hippocampal representations as the neural basis of reorientation behavior.

RESULTS

Spatial Geometry Orients a Reliable Hippocampal Map after Disorientation

To assess the potential contributions of spatial geometry and other visual cues to the recovery of the hippocampal map after disorientation, we recorded 48 place cells from dorsal CA1 as nine mice foraged for randomly scattered chocolate cereal crumbs in a rectangular chamber (Figure 1A). A visual cue that had been previously shown to be discriminable to both oriented and disoriented mice was present along one wall [6]. To disorient the mouse prior to the start of each trial, the mouse was removed from the chamber and placed in a small, lidded cylinder, which

was subjected to four full clockwise and counterclockwise rotations. The mouse was then placed back into the chamber facing a random direction. The spatial geometry defined by the walls of the chamber and the polarizing visual cue were the only potential orienting cues available (see Supplemental Experimental Procedures). Mice foraged in this chamber on 12 consecutive testing trials on a single day.

Place cell rate maps illustrating the spatial activity of example place cells recorded from this rectangular chamber are shown in Figure 1B (see also Figure S1A). As illustrated by these rate maps, the place field of each cell either remained at the same location or rotated 180° to the geometrically equivalent location from trial to trial, in clear contrast to the stability observed in oriented control mice (Figure S1B). This result indicates that the nongeometric cue, which could serve to disambiguate geometrically equivalent facing directions within the chamber, failed to orient the hippocampal map. Rather, chamber geometry alone oriented this map following disorientation.

We quantified this observation by comparing the rate maps of each cell across trials. For each pairwise combination of trials, we first determined the rotation (0°, 90°, 180°, or 270°) that yielded the best match between the two trial rate maps, measured by the pixel-to-pixel cross-correlation. The rectangular rate maps were compressed to squares to make 90° and 270° rotation comparisons possible (Figure 1C). We then calculated the percent of pairwise trial comparisons (66 comparisons for 12 trials) for which each rotation provided the best match, averaging all cells within each animal as the orientations of simultaneously recorded cells may not be independent. The results indicated a striking influence of spatial geometry on the recovered orientation of each cell (Figure 1D). A repeated-measures ANOVA confirmed that not all rotations yielded the best match equally often ($F(1.6,12.6) = 11.1$; $p = 0.003$; Greenhouse-Geisser corrected for sphericity violation). Rather, geometrically consistent rotations by 0° or 180° yielded the best match more often than geometrically inconsistent rotations by 90° or 270° (paired t test: $t(8) = 4.0$; $p = 0.004$), mirroring the rotational symmetry of the rectangular chamber. Moreover, 0° and 180° yielded the best match equally often (paired t test: $t(8) = 0.9$; $p = 0.38$). Similar results were found using an alternative analysis procedure that did not require compression of rate maps, indicating that the effects of spatial geometry are not a product of rate map compression (Figures S1C and S1D). Together, these results suggest that spatial geometry alone determined the recovered orientations of each cell.

The pronounced influence of spatial geometry on the recovered orientations of individual cells suggests that a reliable hippocampal map is recovered across trials. Indeed, after aligning each map based on the best-match rotation, the rate maps of each cell were more similar across trials than expected by chance ($r = 0.69 \pm 0.01$ mean ± SEM; $p < 0.001$; see Experimental Procedures) and remained highly correlated across trials aligned by both geometrically consistent ($r = 0.71 \pm 0.02$) and inconsistent ($r = 0.64 \pm 0.03$) rotations. Notably, the correlations between rate maps aligned by geometrically consistent rotations were significantly higher than the correlations between rate maps aligned by geometrically inconsistent rotations (paired t test: $t(8) = 3.7$; $p = 0.006$), suggesting that geometrically inconsistent rotations may reflect a less stable hippocampal map. Simultaneously recorded cells also tended to orient coherently across trials: the patterns of best-match rotations were more similar than expected by chance for the majority (77 of 115; 67.0%) of simultaneously recorded cell pairs ($p < 0.01$; see Experimental Procedures). Together, these results demonstrate that a reliable and coherent hippocampal map, as observed on similar timescales in oriented mice [40], is recovered following disorientation and that this map is oriented by spatial geometry.

Given the strong influence of geometry on the recovered orientation of a reliable hippocampal map in a rectangular chamber, we next asked whether similar effects of spatial geometry would be observed in chambers of other shapes. Using the same paradigm, we recorded 66 place cells from dorsal CA1 as nine disoriented mice repeatedly foraged in a square chamber over 12 consecutive trials (Figure 2A). The square chamber also contained a discriminable visual cue along one wall that uniquely specified orientations within the chamber [6]. Because the square has 4-fold rotational symmetry, the use of spatial geometry to orient the hippocampal map should yield four possible map orientations across trials, differing by 90° increments.

Place cell rate maps from this square chamber are shown in Figure 2B (see also Figure S1A). For each cell, we again quantified the percent of pairwise trial comparisons for which each rotation (0°, 90°, 180°, or 270°) provided the best match between rate maps (Figure 2C). A repeated-measures ANOVA indicated that the distribution of best-match rotations did not differ from chance ($F(2.6,20.8) = 2.8$; $p = 0.069$; Greenhouse-Geisser corrected), mirroring the rotational symmetry of the chamber. The rate maps of each cell were again more similar across trials after alignment than expected by chance ($r = 0.69 \pm 0.02$; $p < 0.001$). Moreover, the majority (179 of 242; 74.0%) of simultaneously recorded cell pairs oriented coherently across trials ($p < 0.01$). Importantly, the similarity of rate maps across trials and the orientation coherence across cells indicate that the distribution of best-match rotations is not the product of random noise. Rather, this distribution reflects four equally likely orientations of a reliable hippocampal map (see also Figure S1D). These results in a square chamber provide further support for the idea that spatial geometry orients the recovered hippocampal map following disorientation.

We then repeated the same procedure in an isosceles triangular chamber (Figure 2D). If the recovered orientation of the hippocampal map is determined by spatial geometry following disorientation, then a single stable orientation should be observed across trials in this chamber, which lacks rotational symmetry. We recorded 37 place cells from dorsal CA1 as eight disoriented mice repeatedly foraged during 12 consecutive trials. Place cell rate maps from this chamber are shown in Figure 2E (see also Figure S1A). For each cell, we quantified the percent of pairwise trial comparisons for which each rotation (0°, 120°, or 240°) provided the best match between rate maps, first compressing each rate map to an equilateral triangle to make the rotated comparisons possible (Figure 2F). An initial repeated-measures ANOVA indicated that not all rotations yielded the best match equally often ($F(1.0,8.3) = 30.6$; $p < 0.001$; Greenhouse-Geisser corrected). Rather, a rotation by 0° yielded the best match more often than rotations by 120° or 240° (paired t tests: $t(7) = 8.1$, $p < 0.001$, and $t(7) = 7.7$, $p < 0.001$, respectively), consistent with a single stable orientation

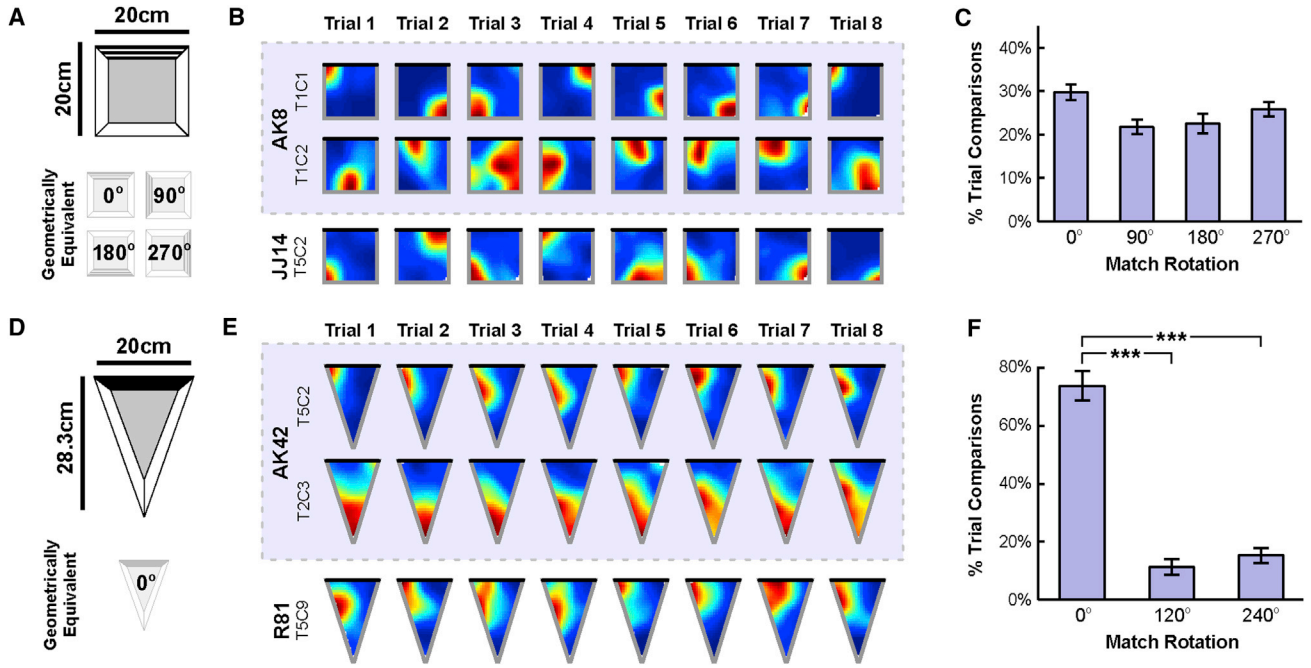

Figure 2. Spatial Geometry Orients a Reliable Hippocampal Map following Disorientation in a Square and Isosceles Triangular Chamber

(A) Schematic of the square chamber and the polarizing visual cue. Note that four rotations of the square chamber, 0°, 90°, 180°, and 270°, result in geometrically equivalent shapes.

(B) Example rate maps from the first eight trials in the square chamber for three place cells, two of which were simultaneously recorded (blue shading). Black line indicates the location of the visual cue.

(C) Distribution of best-match rotations across animals in the square chamber. This distribution did not differ from chance, mirroring the rotational symmetry of the square chamber.

(D) Schematic of the isosceles triangular chamber and the polarizing visual cue. Note that this chamber lacks rotational symmetry.

(E) Example rate maps from the first eight trials in the triangular chamber for three place cells, two of which were simultaneously recorded (blue shading). Black line indicates the location of the visual cue.

(F) Distribution of best-match rotations across animals in the triangular chamber. Only a rotation of 0° yielded the best match more often than chance, mirroring the lack of rotational symmetry of this chamber.

All error bars denote ±1 SEM across animals. See also Figure S1. ***$p < 0.001$.

of a reliable map (see also Figure S1D). Indeed, the rate maps of each cell were more similar across trials than expected by chance, even without any additional alignment ($r = 0.50 \pm 0.04$; $p < 0.001$). Thus, as in the rectangular and square, the orientation of the recovered hippocampal map in the triangle is aligned to the chamber geometry.

Taken together, these results indicate that spatial geometry alone consistently orients the hippocampal map following disorientation. To further test this claim, we calculated the Bayes factor [41, 42] comparing the null hypothesis that best-match rotations were randomly distributed to the alternative hypothesis that best-match rotations were more often consistent with chamber geometry (see Supplemental Experimental Procedures). In the rectangular and triangular chambers, where geometry predicts nonuniform distributions of best-match rotations, we found Bayes factors of 8.97×10^{20} and 1.41×10^{51}, respectively, both of which provide very strong evidence in favor of the alternative hypothesis. To verify that nongeometric cues failed to orient the hippocampal map, we compared the null hypothesis that all geometrically consistent rotations were observed with equal frequency to the alternative hypothesis that these rotations were disambiguated by the nongeometric cue. In both the rectangular and square chambers, where multiple orientations are geometrically equivalent, we found Bayes factors of 1.72 and 0.1, respectively, which together provide evidence in favor of the null hypothesis that nongeometric cues failed to disambiguate geometrically equivalent orientations. Thus, these results provide additional evidence that spatial geometry alone consistently orients the hippocampal map following disorientation.

The Recovered Orientation of the Hippocampal Map Predicts Reorientation Behavior on a Trial-by-Trial Basis

We next investigated whether there was a relationship between the recovered orientation of the hippocampal map and reorientation behavior. To this end, we recorded 42 place cells from dorsal CA1 as seven disoriented mice completed the classic spatial reorientation paradigm, which involves searching for a hidden reward after disorientation. This task thus yielded two potentially related measures of orientation: the orientation of the recovered hippocampal map and the cognitive orientation inferred from search behavior.

The task was conducted in the same rectangular chamber used in the first experiment, except that medicine cups were embedded in the floor near each corner (Figure 3A). These

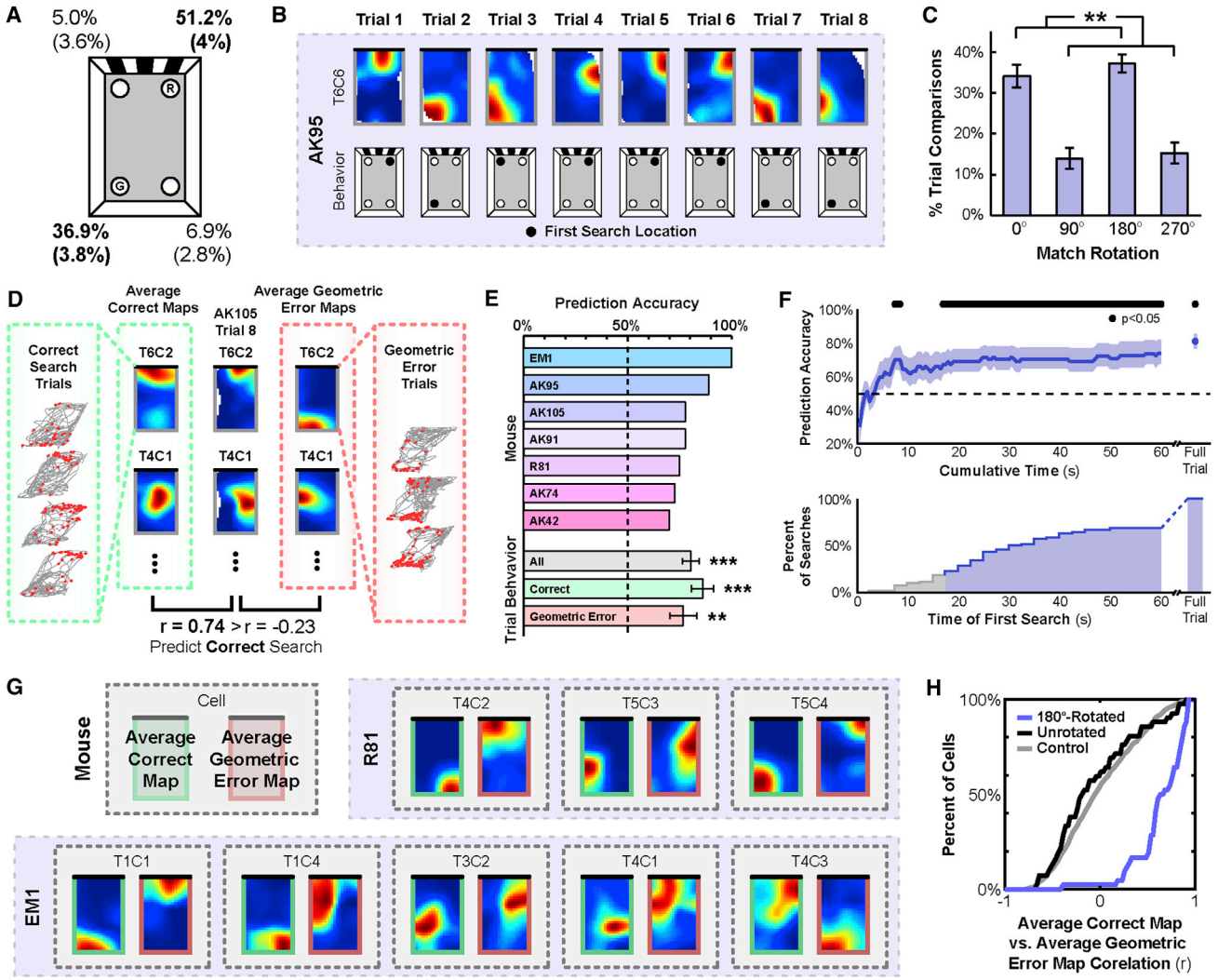

Figure 3. The Orientation of the Recovered Hippocampal Map Predicts Search Behavior during a Spatial Reorientation Task on a Trial-by-Trial Basis

(A) Schematic of the chamber with the rewarded (R) and geometric error (G) locations noted and the corresponding distribution of first searches (mean ± SEM).

(B) Examples of place cell rate maps and search behavior from the first eight trials during the spatial reorientation paradigm.

(C) Distribution of best-match rotations across animals during the spatial reorientation paradigm. Rotations of 0° and 180° most often and equally often yielded the best match, mirroring the rotational symmetry of the chamber.

(D) Schematic of the behavior prediction analysis. To predict behavior on each trial, two average maps were created by combining either all other correct or all other geometric error search trials for each cell. Then, the population vector correlation between the to-be-predicted trial rate maps and each of the average behavior rate maps was calculated. The behavior corresponding to the higher correlation was predicted.

(E) Individual and average prediction accuracy.

(F) Prediction accuracy using only data from cumulatively longer time intervals starting from the beginning of the to-be-predicted trial (top) and the cumulative distribution of the time of first search (bottom).

(G) Example average behavior rate maps, including all trials with the corresponding behavior.

(H) Cumulative distributions of correlations between the average correct map and the average geometric error map, either rotated 180° or unrotated, compared to a shuffled control.

All error bars denote ±1 SEM across animals. See also Figure S2. **p < 0.01; ***p < 0.001.

cups were filled with odor-masked bedding at the beginning of each trial, and the cup to the right of the visual cue was consistently rewarded with buried chocolate cereal crumbs. On each trial (12 per day except for one mouse, who received eight trials per day), the mouse was disoriented as previously described and then released in the chamber. The cup in which the mouse first dug for the buried reward was taken as the measure of search behavior. Each trial continued for at least 3 min until the mouse found the reward and the chamber was adequately sampled. To ensure that search behavior reflected memory for the reward location and not simply random searching, this task was repeated each day until a performance criterion was met. Data

were analyzed only for the 1st day on which at least 66% of first searches were at the correct or geometric error locations (range 1–3 days).

We first confirmed that the pattern of search behavior we observed with this task replicated the typical pattern of reorientation behavior previously characterized with this paradigm [6]. Figure 3A shows the distribution of first search locations for days meeting the performance criterion. As guaranteed by our performance criterion, the majority of first searches were made at either the correct or geometric error locations. Importantly, there was no significant difference in search preference between these two locations (paired t test: $t(6) = 2.0$; $p = 0.09$), demonstrating that search behavior was primarily guided by spatial geometry.

Next, we confirmed that spatial geometry also determined the orientation of the recovered hippocampal map during this task, as was the case during free foraging. Figure 3B shows place cell rate maps during this task. For each cell, we again quantified the percent of pairwise trial comparisons for which each rotation (0°, 90°, 180°, or 270°) provided the best match between rate maps (Figure 3C). A repeated-measures ANOVA indicated that not all rotations yielded the best match equally often ($F(1.4,8.2) = 22.5$; $p = 0.002$; Greenhouse-Geisser corrected). Rather, rotations by 0° or 180° yielded the best match more often than rotations by 90° or 270° (paired t test: $t(6) = 4.6$; $p = 0.004$; Bayes factor of 7.14×10^{11}; very strong evidence for geometrically consistent rotations). Furthermore, 0° and 180° yielded the best match equally often (paired t test: $t(6) = 1.5$; $p = 0.18$; Bayes factor of 0.015; evidence for the null hypothesis that geometrically consistent rotations were observed with equal frequency), suggesting that spatial geometry alone determined the recovered orientations of each cell (see also Figures S2A and S2B). When aligned by their best-match rotations, the rate maps of each cell were more similar across trials than would be expected by chance ($r = 0.70 \pm 0.02$; $p < 0.001$) and remained highly correlated across trials aligned by both geometrically consistent ($r = 0.72 \pm 0.03$) and inconsistent ($r = 0.62 \pm 0.05$) rotations, though the difference between these correlations was again significant (paired t test: $t(6) = 3.1$; $p = 0.021$). Lastly, the majority (80 of 149; 53.7%) of simultaneously recorded cell pairs were again oriented coherently across trials ($p < 0.01$). These results replicate the pattern we observed in the rectangular chamber during free foraging: the recovered orientation of the hippocampal map is primarily informed by spatial geometry.

Because both the hippocampal map orientation and search behavior were guided by spatial geometry, we next directly addressed the potential relationship between the two. We hypothesized that the orientation of the recovered hippocampal map would predict reorientation behavior on a trial-by-trial basis. Because our performance criterion limited the number of nongeometric errors, we focused the main analyses only on geometrically consistent search trials (see Figure S2C for supplemental analysis of the nongeometric error trials). We first attempted to predict correct and geometric error searches on the basis of the recovered hippocampal map. To do so, we created two average rate maps for each cell, one of correct searches and one of geometric error searches, by combining all trials during which each behavior was made, excluding the to-be-predicted trial (Figure 3D). We then computed the population vector correlation between the to-be-predicted trial rate maps and the average rate maps derived from correct and geometric error searches and predicted the behavior corresponding to the higher correlation. Using this method, search prediction accuracy for each animal exceeded 50%, with the average prediction accuracy across animals significantly above chance (80.3% ± 4.0%; t test against 50%: $t(6) = 7.6$; $p < 0.001$; Figure 3E). Moreover, both correct and geometric error trials were reliably predicted (t test against 50%: $t(6) = 6.7$, $p < 0.001$, and $t(6) = 4.13$, $p = 0.006$, respectively), with no significant difference between the prediction accuracy for these two searches (paired t test: $t(6) = 1.0$; $p = 0.35$).

We next asked whether the recovered hippocampal map consistently predicted search behavior before the actual search behavior was performed. To do so, we again predicted search behavior on each trial using the average map method but only included data from incrementally longer time intervals starting from the beginning of the to-be-predicted trial (Figure 3F). This analysis revealed that search behavior could be reliably predicted on the basis of as little as the first 17 s of trial data, earlier than 81.4% of first searches (median time of first search: 32.5 s). Interestingly, during the first 17 s, the animals tended to explore the perimeter of the chamber (Figure S2D), suggesting that the animals often had both visual and tactile experience with the chamber geometry prior to making a decision. Moreover, when only data prior to the first search were included for each trial, prediction accuracy remained high (72.5% ± 8.3%; $t(6) = 2.7$; $p = 0.035$). Together, these results demonstrate that reliable and predictive hippocampal maps emerge as early as within the first 17 s of the trial, often long before the animal first digs for the reward, suggesting that reorientation is a rapid process.

Finally, we confirmed that the hippocampal maps underlying correct and geometric search behavior were in fact 180° rotations of one another. For each cell, we again created average maps for both behaviors, now including all trials (Figure 3G; see also Figure S2E). Next, we computed the correlation between the average correct map and the 180°-rotated average geometric error map for each cell. We then compared the distribution of these correlation values against a control distribution created by randomly shuffling the average geometric error maps across cells 100 times. Average correct maps were significantly more correlated with the 180°-rotated average geometric error maps than expected by chance (one-sample Kolmogorov-Smirnov test: $D = 0.67$; $p < 0.001$; Figure 3H). By contrast, average correct maps were not significantly correlated with the unrotated average geometric error maps (one-sample Kolmogorov-Smirnov test: $D = 0.15$; $p = 0.24$; Figure 3H). Together, these results indicate that the recovered orientation of the hippocampal map, informed by spatial geometry, reliably predicts reorientation search behavior on a trial-by-trial basis.

DISCUSSION

There were two primary results of this study. First, we found that spatial geometry consistently oriented the recovered hippocampal maps of disoriented mice in three differently shaped chambers (rectangle, square, and isosceles triangle). From trial to trial, the orientation of the map varied in a manner that reflected the

rotational symmetry of each chamber, despite the presence of nongeometric cues that could potentially disambiguate geometrically equivalent orientations. Second, in a classic reorientation task, we found that the recovered orientation of the hippocampal map predicted goal-directed search behavior on a trial-by-trial basis. These results demonstrate for the first time that spatial geometry is used to realign the hippocampal map after disorientation and that the resulting alignment of the map controls navigational behavior.

These findings have important implications for the ongoing debate over the computations underlying spatial reorientation [2, 3, 8, 9, 12–14, 18, 43]. Allocentric theories claim that reorientation is accomplished by aligning the cognitive map to the surrounding environment to recover one's heading [4, 11, 13–15]. Egocentric theories, on the other hand, hold that navigation after disorientation reflects the use of a view-matching strategy that does not require heading to be re-established [16–18]. Our data provide clear evidence for the involvement of the hippocampal map in reorientation, thus supporting the allocentric view. Moreover, the fact that the recovered hippocampal map aligned exclusively to chamber geometry is consistent with the claim that environmental shape plays a privileged role in reorientation. Interestingly, other studies have reported circumstances in which nongeometric cues guide reorientation behavior, such as after oriented, aversive, or extensive experience [32, 33, 35, 44] or when there is a configuration of multiple distal cues [39]; whether the hippocampal map is exclusively aligned by spatial geometry under these other circumstances remains to be tested. However, the fact that we observed a tight correspondence between the geometry of the chamber, the recovered alignment of the hippocampal map, and the search locations of the animals strongly suggests that the reliance on geometry observed in many previous behavioral studies of reorientation is a consequence of the geometric reorientation of the hippocampal map.

At a circuit level, the mechanism by which spatial geometry orients the hippocampal map is currently unknown. This mechanism may involve HD cells, which are active when the navigator faces a particular direction. HD cells are located in a number of regions that interact, directly or indirectly, with the hippocampus, including the medial entorhinal cortex [45], retrosplenial cortex [46], postsubiculum [47], and anterodorsal thalamic nuclei [48]. The preferred directions of HD cells are typically found to be strongly coupled to the alignment of the hippocampal map [32], and spatial geometry is thought to play an important role in determining these preferred directions under disoriented conditions [38, 39]. Thus, the hippocampal map may be oriented by HD input in a bottom-up manner [37, 49]. Consistent with this view, lesions to the postsubiculum severely impair the recovery of an oriented hippocampal map [50]. On the other hand, lesions to the anterodorsal thalamic nuclei yield comparatively weaker deficits [50] and disjunctions between HD firing in this latter region and reorientation behavior have been reported [36]. Thus, an alternative possibility is that the reorientation signal we observe may instead originate within the hippocampus itself, which in turn updates HD representations in other regions [49].

Because the hippocampal map is often specific to each environment [26], recovery of this map after disorientation must involve more than simply re-establishing heading: the proper map reflecting the current environment must also be recovered. We recently demonstrated that the processes of identifying the environment and recovering heading after disorientation are behaviorally dissociable, with differential sensitivities to spatial geometry and nongeometric visual cues [6]. Specifically, in a two-chamber reorientation paradigm where disoriented mice were required to both re-establish heading and identify the current chamber, nongeometric visual cues were used for chamber identification but simultaneously ignored for determining heading. Thus, nongeometric cues might play an important role in determining which cognitive map is recovered, even though they are subsequently ignored when re-establishing the alignment of that hippocampal map. Critically, these earlier results suggest that the exclusive alignment of the hippocampal map to chamber geometry observed here does not stem from a failure to notice the nongeometric cues. Rather, spatial geometry plays a unique role in re-establishing heading representations that surpasses mere salience.

In sum, we have shown that a reliable hippocampal map is recovered following disorientation, the orientation of which is determined by the shape of the navigable space. Furthermore, we have shown that the orientation of this map predicts search behavior on a trial-by-trial basis, linking reorientation behavior to allocentric spatial representations. Together, these results provide a critical first step toward understanding the physiological mechanisms that allow navigators to regain their bearings after becoming lost.

EXPERIMENTAL PROCEDURES

Best-Match Rotation Analysis

In all experiments, a best-match rotation analysis was used to quantify the orientation, reliability, and coherence of the hippocampal map. First, rectangular or isosceles triangular rate maps were compressed to squares or equilateral triangles, respectively. Next, for each cell and each pair of trials, the rotation of the trial A rate map (square/rectangle: 0°, 90°, 180°, or 270°; triangle: 0°, 120°, or 240°) that maximized the pixel-to-pixel correlation to the trial B rate map was computed. The percent of pairwise trial comparisons for which each rotation yielded the best match was then calculated for each cell. These percentages were then averaged within each animal as the orientations of simultaneously recorded cells are likely not independent.

Rate Map Similarity Analysis

To measure the similarity of rate maps across trials for each cell, the best-match rotation correlation value was computed for each pair of trial comparisons and then averaged across all comparisons. To test significance, these correlation values were averaged across all cells, and this correlation value was compared to a shuffled control generated by randomly shuffling rate maps across cells and trials prior to computing the best-match rotations (1,000 iterations).

Orientation Coherence Analysis

To measure the orientation coherence of simultaneously recorded cell pairs, the pattern of best-match rotations across all pairwise trial comparisons for both cells was compared. The similarity between these patterns was quantified as the proportion of comparisons for which the same rotation yielded the best match. Trial comparisons for which at least one cell in the pair was inactive were excluded. To assess the significance of this orientation coherence, pattern similarity was compared to a shuffled control created by shuffling the best-match rotation pattern order for each cell independently. A cell pair was considered significantly coherent if its similarity exceeded the 99th percentile of 1,000 iterations of this shuffled control. Note that this method is

overly conservative and thus establishes a lower bound on observed coherence (see also Supplemental Experimental Procedures).

Statistics

All parametric statistical tests are named where appropriate. All t tests were two-tailed. For a complete description of all Bayes factors and nonparametric tests, see the Supplemental Experimental Procedures.

SUPPLEMENTAL INFORMATION

Supplemental Information includes two figures and Supplemental Experimental Procedures and can be found with this article online at http://dx.doi.org/10.1016/j.cub.2016.11.046.

AUTHOR CONTRIBUTIONS

A.T.K., J.B.J., R.A.E., and I.A.M. designed research. A.T.K. and J.B.J. performed research. A.T.K. and J.B.J. analyzed the data. A.T.K., J.B.J., R.A.E., and I.A.M. wrote the manuscript.

ACKNOWLEDGMENTS

This work was supported by NIH grant EY022350 (R.A.E.), NSF grant SBE-1041707, NSF CAREER Award 1565410 (I.A.M.), NSF IGERT grant 0966142 (A.T.K. and J.B.J.), and an NSF Graduate Research Fellowship (J.B.J.).

Received: July 29, 2016
Revised: October 28, 2016
Accepted: November 23, 2016
Published: January 12, 2017

REFERENCES

1. Mittelstaedt, M.-L., and Mittelstaedt, H. (1980). Homing by path integration in a mammal. Naturwissenschaften *67*, 566–567.
2. Cheng, K., Huttenlocher, J., and Newcombe, N.S. (2013). 25 years of research on the use of geometry in spatial reorientation: a current theoretical perspective. Psychon. Bull. Rev. *20*, 1033–1054.
3. Cheng, K., and Newcombe, N.S. (2005). Is there a geometric module for spatial orientation? Squaring theory and evidence. Psychon. Bull. Rev. *12*, 1–23.
4. Cheng, K. (1986). A purely geometric module in the rat's spatial representation. Cognition *23*, 149–178.
5. Lee, S.A., Spelke, E.S., and Vallortigara, G. (2012). Chicks, like children, spontaneously reorient by three-dimensional environmental geometry, not by image matching. Biol. Lett. *8*, 492–494.
6. Julian, J.B., Keinath, A.T., Muzzio, I.A., and Epstein, R.A. (2015). Place recognition and heading retrieval are mediated by dissociable cognitive systems in mice. Proc. Natl. Acad. Sci. USA *112*, 6503–6508.
7. Hermer, L., and Spelke, E.S. (1994). A geometric process for spatial reorientation in young children. Nature *370*, 57–59.
8. Wang, R., and Spelke, E. (2002). Human spatial representation: insights from animals. Trends Cogn. Sci. *6*, 376.
9. Lee, S.A., and Spelke, E.S. (2010). Two systems of spatial representation underlying navigation. Exp. Brain Res. *206*, 179–188.
10. Burgess, N. (2006). Spatial memory: how egocentric and allocentric combine. Trends Cogn. Sci. *10*, 551–557.
11. Miller, N.Y., and Shettleworth, S.J. (2007). Learning about environmental geometry: an associative model. J. Exp. Psychol. Anim. Behav. Process. *33*, 191–212.
12. Sheynikhovich, D., Chavarriaga, R., Strösslin, T., Arleo, A., and Gerstner, W. (2009). Is there a geometric module for spatial orientation? Insights from a rodent navigation model. Psychol. Rev. *116*, 540–566.
13. Learmonth, A.E., Newcombe, N.S., Sheridan, N., and Jones, M. (2008). Why size counts: children's spatial reorientation in large and small enclosures. Dev. Sci. *11*, 414–426.
14. Gallistel, C.R. (1990). The Organization of Learning (Bradford Books/MIT Press).
15. Doeller, C.F., King, J.A., and Burgess, N. (2008). Parallel striatal and hippocampal systems for landmarks and boundaries in spatial memory. Proc. Natl. Acad. Sci. USA *105*, 5915–5920.
16. Zeil, J., Hofmann, M.I., and Chahl, J.S. (2003). Catchment areas of panoramic snapshots in outdoor scenes. J. Opt. Soc. Am. A Opt. Image Sci. Vis. *20*, 450–469.
17. Pecchia, T., and Vallortigara, G. (2010). View-based strategy for reorientation by geometry. J. Exp. Biol. *213*, 2987–2996.
18. Stürzl, W., Cheung, A., Cheng, K., and Zeil, J. (2008). The information content of panoramic images I: The rotational errors and the similarity of views in rectangular experimental arenas. J. Exp. Psychol. Anim. Behav. Process. *34*, 1–14.
19. Packard, M.G., and McGaugh, J.L. (1996). Inactivation of hippocampus or caudate nucleus with lidocaine differentially affects expression of place and response learning. Neurobiol. Learn. Mem. *65*, 65–72.
20. Packard, M.G., and McGaugh, J.L. (1992). Double dissociation of fornix and caudate nucleus lesions on acquisition of two water maze tasks: further evidence for multiple memory systems. Behav. Neurosci. *106*, 439–446.
21. O'Keefe, J., and Nadel, L. (1978). The Hippocampus as a Cognitive Map (Oxford University Press).
22. Barnes, T.D., Kubota, Y., Hu, D., Jin, D.Z., and Graybiel, A.M. (2005). Activity of striatal neurons reflects dynamic encoding and recoding of procedural memories. Nature *437*, 1158–1161.
23. Iaria, G., Petrides, M., Dagher, A., Pike, B., and Bohbot, V.D. (2003). Cognitive strategies dependent on the hippocampus and caudate nucleus in human navigation: variability and change with practice. J. Neurosci. *23*, 5945–5952.
24. Maguire, E.A., Burgess, N., Donnett, J.G., Frackowiak, R.S., Frith, C.D., and O'Keefe, J. (1998). Knowing where and getting there: a human navigation network. Science *280*, 921–924.
25. O'Keefe, J. (1976). Place units in the hippocampus of the freely moving rat. Exp. Neurol. *51*, 78–109.
26. Alme, C.B., Miao, C., Jezek, K., Treves, A., Moser, E.I., and Moser, M.-B. (2014). Place cells in the hippocampus: eleven maps for eleven rooms. Proc. Natl. Acad. Sci. USA *111*, 18428–18435.
27. Zhang, S.-J., Ye, J., Miao, C., Tsao, A., Cerniauskas, I., Ledergerber, D., Moser, M.-B., and Moser, E.I. (2013). Optogenetic dissection of entorhinal-hippocampal functional connectivity. Science *340*, 1232627.
28. Witter, M.P., Groenewegen, H.J., Lopes da Silva, F.H., and Lohman, A.H. (1989). Functional organization of the extrinsic and intrinsic circuitry of the parahippocampal region. Prog. Neurobiol. *33*, 161–253.
29. Muller, R.U., and Kubie, J.L. (1987). The effects of changes in the environment on the spatial firing of hippocampal complex-spike cells. J. Neurosci. *7*, 1951–1968.
30. O'Keefe, J., and Speakman, A. (1987). Single unit activity in the rat hippocampus during a spatial memory task. Exp. Brain Res. *68*, 1–27.
31. Jeffery, K.J., Donnett, J.G., Burgess, N., and O'Keefe, J.M. (1997). Directional control of hippocampal place fields. Exp. Brain Res. *117*, 131–142.
32. Knierim, J.J., Kudrimoti, H.S., and McNaughton, B.L. (1995). Place cells, head direction cells, and the learning of landmark stability. J. Neurosci. *15*, 1648–1659.
33. Dudchenko, P.A., Goodridge, J.P., and Taube, J.S. (1997). The effects of disorientation on visual landmark control of head direction cell orientation. Exp. Brain Res. *115*, 375–380.

34. Taube, J.S., Muller, R.U., and Ranck, J.B., Jr. (1990). Head-direction cells recorded from the postsubiculum in freely moving rats. II. Effects of environmental manipulations. J. Neurosci. *10*, 436–447.

35. Clark, B.J., and Taube, J.S. (2011). Intact landmark control and angular path integration by head direction cells in the anterodorsal thalamus after lesions of the medial entorhinal cortex. Hippocampus *21*, 767–782.

36. Golob, E.J., Stackman, R.W., Wong, A.C., and Taube, J.S. (2001). On the behavioral significance of head direction cells: neural and behavioral dynamics during spatial memory tasks. Behav. Neurosci. *115*, 285–304.

37. Golob, E.J., and Taube, J.S. (1997). Head direction cells and episodic spatial information in rats without a hippocampus. Proc. Natl. Acad. Sci. USA *94*, 7645–7650.

38. Knight, R., Hayman, R., Lin Ginzberg, L., and Jeffery, K. (2011). Geometric cues influence head direction cells only weakly in nondisoriented rats. J. Neurosci. *31*, 15681–15692.

39. Clark, B.J., Harris, M.J., and Taube, J.S. (2012). Control of anterodorsal thalamic head direction cells by environmental boundaries: comparison with conflicting distal landmarks. Hippocampus *22*, 172–187.

40. Kentros, C.G., Agnihotri, N.T., Streater, S., Hawkins, R.D., and Kandel, E.R. (2004). Increased attention to spatial context increases both place field stability and spatial memory. Neuron *42*, 283–295.

41. Gallistel, C.R. (2009). The importance of proving the null. Psychol. Rev. *116*, 439–453.

42. Dienes, Z. (2011). Bayesian versus orthodox statistics: which side are you on? Perspect. Psychol. Sci. *6*, 274–290.

43. Spelke, E.S., and Kinzler, K.D. (2007). Core knowledge. Dev. Sci. *10*, 89–96.

44. Golob, E.J., and Taube, J.S. (2002). Differences between appetitive and aversive reinforcement on reorientation in a spatial working memory task. Behav. Brain Res. *136*, 309–316.

45. Sargolini, F., Fyhn, M., Hafting, T., McNaughton, B.L., Witter, M.P., Moser, M.-B., and Moser, E.I. (2006). Conjunctive representation of position, direction, and velocity in entorhinal cortex. Science *312*, 758–762.

46. Chen, L.L., Lin, L.H., Green, E.J., Barnes, C.A., and McNaughton, B.L. (1994). Head-direction cells in the rat posterior cortex. I. Anatomical distribution and behavioral modulation. Exp. Brain Res. *101*, 8–23.

47. Taube, J.S., Muller, R.U., and Ranck, J.B., Jr. (1990). Head-direction cells recorded from the postsubiculum in freely moving rats. I. Description and quantitative analysis. J. Neurosci. *10*, 420–435.

48. Taube, J.S. (1995). Head direction cells recorded in the anterior thalamic nuclei of freely moving rats. J. Neurosci. *15*, 70–86.

49. Golob, E.J., and Taube, J.S. (1999). Head direction cells in rats with hippocampal or overlying neocortical lesions: evidence for impaired angular path integration. J. Neurosci. *19*, 7198–7211.

50. Calton, J.L., Stackman, R.W., Goodridge, J.P., Archey, W.B., Dudchenko, P.A., and Taube, J.S. (2003). Hippocampal place cell instability after lesions of the head direction cell network. J. Neurosci. *23*, 9719–9731.

Current Biology, Volume *27*

Supplemental Information

Environmental Geometry Aligns the Hippocampal Map during Spatial Reorientation

Alex T. Keinath, Joshua B. Julian, Russell A. Epstein, and Isabel A. Muzzio

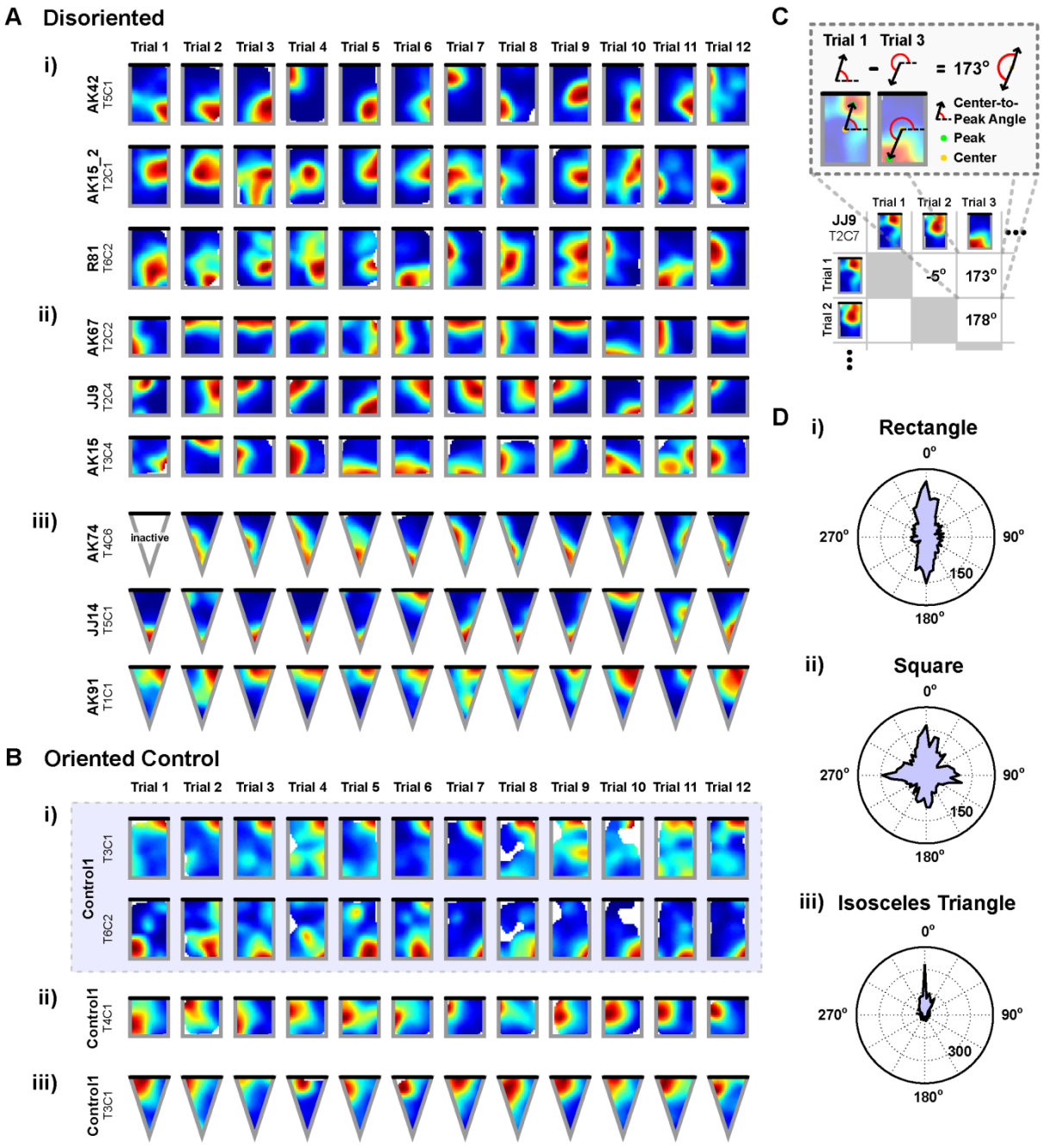

Figure S1. Supplementary results for the foraging experiments. Related to Figures 1 and 2.

Additional examples of place cell rate maps from (A) 3 disoriented mice and (B) one oriented control mouse for all 12 trials of foraging in: i) the rectangular, ii) the square, and iii) the isosceles triangular chambers. The black line on the edge of the chamber indicates the location of the nongeometric visual cue. (C) Schematic of the center-to-peak angle analysis. First, for each cell and trial the angle from the center of the environment to the pixel with maximum firing was measured. Then for each pair of trials within each cell, the difference between the center-to-peak angles was computed. Finally, a histogram representing the distribution of these center-to-peak angles across all cells and pairwise trial comparisons was created. Note that this analysis does not rely on compression of rate maps. (D) Polar histograms resulting from the center-to-peak angle analysis of disoriented mice in: i) the rectangular, ii) the square, and iii) the isosceles triangular chambers during foraging. Radius indicated in the lower right of each histogram. Note that the maxima of these distributions mirror the rotational symmetry of each chamber.

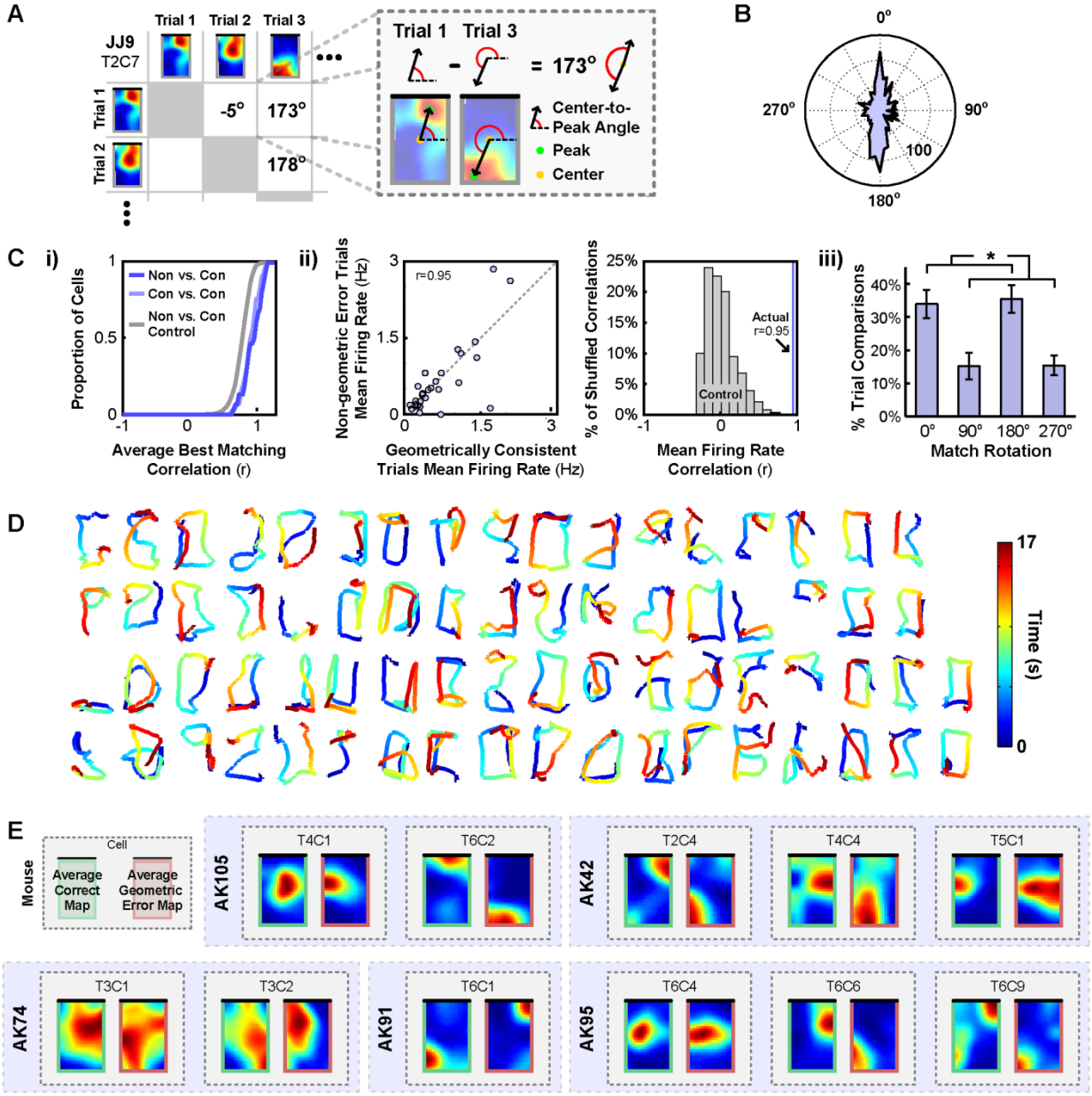

Figure S2. Supplementary results for the spatial reorientation task experiment. Related to Figure 3.

(A) Schematic of the center-to-peak angle analysis as in Figure S1C. First, for each cell and trial the angle from the center of the environment to the pixel with maximum firing was measured. Then for each pair of trials within each cell, the difference between the center-to-peak angles was computed. Finally, a histogram representing the distribution of these center-to-peak angles across all cells and pairwise trial comparisons was created. Note that this analysis does not rely on compression of rate maps.

(B) Polar histograms resulting from the center-to-peak angle analysis in the rectangular chamber during the spatial reorientation task. Radius indicated in the lower right of the histogram. Note that the maxima of this distribution mirror the rotational symmetry of the chamber.

(C) Although nongeometric searches (searches at locations other than the correct and geometric error locations) were rare, all but one mouse made at least one nongeometric error (4 mice made 1 nongeometric error, 2 mice made 2

nongeometric errors). We assessed the potential hippocampal contribution to nongeometric error trials by comparing the hippocampal maps between nongeometric error and geometrically consistent search trials in three different ways:

i) To assess whether place cells exhibited similar maps on geometrically consistent (Con) and nongeometric error (Non) trials, we first computed the similarity between geometrically consistent and nongeometric error rate maps. The average best match correlation values for comparisons between geometrically consistent and nongeometric error trial rate maps was high (Non vs. Con; $r=0.728\pm0.024$), exceeding the shuffled control ($p<0.001$; see Supplementary Methods below). Moreover, the similarity between geometrically consistent and nongeometric error trial rate maps was not different from the similarity between two geometrically consistent trial rate maps (Con vs. Con; $r=0.70\pm0.018$; paired t-test: $t(29)=0.68$, $p=0.50$). These results indicate that the preferred firing locations of place cells did not globally remap to new locations during nongeometric error trials.

ii) Given that the preferred firing locations of cells did not remap, we next asked whether rate differences might underlie nongeometric error trials. Mean firing rates during nongeometric error and geometrically consistent trials were highly correlated ($r=0.95$, $p<0.001$). This correlation exceeded its shuffled control generated by shuffling the nongeometric error trial mean firing rates across cells 1000 times ($p<0.001$). These results suggest that no reliable rate remapping was observed during nongeometric error trials.

iii) Because similar rate maps and firing rates were observed during nongeometric error and geometrically consistent search trials, we lastly asked whether 90° or 270° map rotations might underlie these nongeometric errors. To do so, we computed the percent of pairwise trial comparisons for which each rotation (0°, 90°, 180°, or 270°) yielded the best match, restricted to comparisons of nongeometric error trial rate maps to geometrically consistent trial rate maps. An initial repeated measures ANOVA indicated that not all rotations yielded the best match equally often ($F(1.6,8.1)=6.2$, $p=0.027$; Greenhouse-Geisser corrected). Rather, rotations by 0° or 180° yielded the best match more often than rotations by 90° or 270° (paired t-test: $t(5)=2.9$, $p=0.033$), and best match rotations of 0° and 180° rotations occurred with similar frequency (paired t-test: $t(5)=0.3$, $p=0.77$). These results indicate that nongeometric error searches were not linked to 90° or 270° rotations of the hippocampal map. Rather, the spatial geometry alone continued to orient hippocampal representations on nongeometric error trials. Therefore, the orientation of the hippocampal map did not dictate the behavior of the animal during error trials. Error bars denote mean ± 1 SEM. *$p<0.05$

The similarity of the rate maps, firing rates, and distribution of preferred orientations between geometrically consistent and nongeometric error searches suggests that nongeometric errors may be the product of extra-hippocampal circuits. Nevertheless, because nongeometric errors were very rare, we refrain from drawing strong conclusions about the mechanism underlying these errors.

(D) Search paths during the first 17 s of each trial, at which point the hippocampal map is predictive of search behavior. Note that on most trials the animals spend the first seconds exploring the perimeter of the chamber.

(E) Example average correct and average geometric error maps from all mice not shown in Figure 3. All analyzed trials during the spatial reorientation task are included in the average maps. Blue shading indicates simultaneously recorded cells. The black line on the edge of the chamber indicates the location of the nongeometric visual cue.

Supplemental Experimental Procedures

Subjects

Naive male mice 2-6 months of age (C57Bl/6, Jackson Laboratory, Bar Harbor, ME) were housed individually on a 12-hour light/dark cycle. To increase motivation to participate in all experiments, the mice were maintained at 85%-90% of their *ad libitum* weight. All experiments were carried out during the light portion of the light/dark cycle, and in accordance with NIH guidelines and approved by the Institution of Animal Care and Use Committee of the University of Pennsylvania and the University of Texas at San Antonio.

Experimental Protocol

Chambers. The rectangular chamber consisted of four white walls (short walls 20 cm x long walls 30 cm x height 35 cm), with three evenly-spaced 4 cm wide vertically-oriented black stripes spanning one short wall serving as the nongeometric visual cue. The square chamber consisted of four white walls (all walls 20 cm x height 35 cm), with three evenly-spaced 4 cm wide horizontally-oriented black stripes spanning one wall serving as the nongeometric visual cue. The isosceles triangular chamber consisted of two white walls (long walls 30 cm x height 35cm), with one solid black wall (short wall 20 cm x height 35 cm) serving as the nongeometric visual cue. Previous experiments have demonstrated that both oriented and disoriented mice can easily discriminate with these nongeometric visual cues [S1]. During all experiments, these chambers were surrounded by a large white cylinder (diameter 70 cm x height 70 cm) and a black curtain to eliminate distal visual cues.

Trial Protocol. Trial structure was similar for all experiments. Prior to each trial, the mouse was placed in a PVC cylinder (diameter 9 cm x height 30 cm) with a detachable base and lid for disorientation. The chamber was vacuumed, wiped down with ethanol to eliminate potential odor cues, and rotated 90° clockwise relative to the previous trial orientation to ensure that the hippocampal map did not track any external cues. To disorient the mouse, the experimenter rotated the cylinder on a turntable four full revolutions clockwise and then again counterclockwise (~180°/sec). The mouse was then immediately placed in the center of the chamber, and the base of the disorientation cylinder was removed so that the mouse stood on the floor of the chamber still encapsulated by the lidded disorientation cylinder. The disorientation cylinder was removed, and the mouse could freely move about the chamber. From the end of disorientation to release in the chamber took ~15 s. Once the trial criteria were met, the mouse was removed, placed back in the disorientation cylinder, and allowed to rest for ~2 min before the beginning of the next trial. A white noise generator was placed above the chamber throughout all experiments to mask any potential distal sound cues. Trial protocol was the same for the oriented control mouse, except that the mouse was never disoriented, held in their home cage between trials, and the chamber was not rotated between trials.

Foraging experiments. During foraging experiments, neural activity was recorded from right dorsal CA1 as disoriented mice (and one oriented control mouse) foraged for small amounts of a food reward (crushed up Kellogg's Cocoa Krispies) scattered throughout the entire chamber prior to the start of each trial. Mice completed one experimental session a day for up to three days, each of which consisted of 12 consecutive trials. Each session took place in one of the three chambers. During each trial, mice foraged for at least three minutes until the chamber was adequately sampled.

Spatial reorientation task experiment. Two days prior to the beginning of the recording, mice were shaped to dig for a food reward buried in a medicine cup placed in their home cage. Once hippocampal cells were identified and the quality of the clusters was checked (see below Electrophysiology), neural activity was recorded from the right dorsal CA1 area as disoriented mice completed a traditional spatial reorientation task. The task consisted of 12 trials per day (one mouse, EM1, received 8 trials per day) in the rectangular chamber containing four medicine cups embedded in the floor near each corner. All medicine cups were filled to the brim with scented bedding (cumin or ginger mixed with regular bedding). For any given animal, the same scent was used for all trials. The right cup nearest the nongeometric visual cue was consistently rewarded on each trial with the buried food reward. On each trial the mouse was disoriented and then released in the chamber to search for the buried reward. The cup in which the mouse first dug was recorded as the measure of search behavior. The mouse remained in the chamber for at least three minutes until the chamber was adequately sampled and the reward was retrieved. To shape learning, the reward was exposed on the first two trials of the first day. These trials were excluded from subsequent analysis. To ensure that search behavior reflected memory for the reward location and not simply random searching, this task was repeated each day until a performance criterion was met. Specifically, for each mouse, data were analyzed only for the first day during which at least 66% of searches were at the correct or geometric error locations (range 1 to 3

days; Criteria was met on Day 1 for most mice, except AK74 (Day 2) and EM1 (Day 3)). This criteria was established prior to recording on the basis of pilot results from [S1], and all mice exceeded this criteria and achieved an accuracy of at least 75% on the analyzed day.

Order of experimental conditions. To maximize the amount of electrophysiological data collected, the majority of mice participated in multiple experimental conditions. The table below lists the order in which each mouse completed each experiment. There were no systematic increases or decreases in the stability of the hippocampal map within any animal across chambers or experiments. However, behavioral prediction accuracy in the spatial reorientation task may be related to prior experience with disorientation or environments, as prediction accuracy was highest among animals that did not experience any other experimental conditions. Nevertheless, we refrain from drawing strong conclusions about this relationship because of the limited number of animals run in each order.

	Foraging			Behavior
Mouse Name	Rectangle	Square	Triangle	Rectangle
AK8	1	2		
JJ9	1	2		
AK15	1	2	3	
AK15_2	1	2	3	
JJ14	1	2	3	
AK67	1	2	3	
AK42	1	2	3	4
R81	1	2	3	4
AK74	3	4	1	2
AK91			1	2
AK95				1
AK105				1
EM1				1
Control1	1	2	3	

Surgery

Mice were anesthetized with a mixture of ketamine (100 mg/kg) and xylazine (10 mg/kg) administered intraperitoneally (0.1 ml/kg) and placed flat on a stereotaxic frame (David Kopf Instruments). They were then implanted with drivable 6-tetrode microdrives above the right dorsal hippocampus (from Bregma (in mm): AP, -1.7; ML, -1.6; DV, -1.0). A ground wire was connected to a screw placed on the contralateral side of the skull above the occipital lobe. The headstages were affixed to the skulls with cyanoacrylate and dental cement.

Electrophysiology

Beginning one week after surgery, neural activity from each tetrode was screened daily. The search for cells was conducted in a circular chamber (diameter 35cm x height 35cm). The headstage was connected to a tethered unity gain amplifier with green and red LEDs for tracking the position of the mouse. Units were amplified using a 32-channel amplifier (Neuralynx), and electrical signals were amplified between 2,500 and 10,000 times and filtered between 400-9,000 Hz. The amplifier output was digitized at 30.3 kHz. The position of the mouse and electrophysiological data were recorded by Cheetah Data Acquisition software (Neuralynx). The tetrode bundle was

slowly advanced by 15-20 μm steps per day into recording position, lowering the tetrodes in small steps to minimize electrode drift [S2,S3]. Pyramidal cells were identified by their characteristic firing patterns [S4]. After completion of an experimental session, units were cluster cut and analyzed using MClust software (developed by A. David Redish, University of Minnesota). Cells were only accepted for analysis if they formed isolated Gaussian clusters with minimal overlap with surrounding cells and noise. Cells were cut simultaneously from all concatenated trials recorded on the same day, without knowledge of the trials from which they originated to eliminate any potential bias in spike sorting. No attempt was made to track the same cells across days. All further analyses were carried out offline in MATLAB using custom-written scripts.

Analyses

Inclusion criteria. Only data from periods of movement in which the velocity of the mouse exceed 2cm/s were included in the analysis. Only cells firing at least 15 spikes during periods of movement during a trial were included in the analysis of that trial.

Rate maps. Rate maps for each cell were created by first binning the chamber into 1 cm x 1 cm pixels, and counting the number of spikes and the amount of time the mouse spent in each pixels. Both the spike map and the time map were then smoothed with an isometric Gaussian kernel with a standard deviation of 3 cm. The final place field map was then the result of the smoothed spike map divided by the smoothed time map. Only pixels sampled for at least 0.05sec after smoothing were considered sampled.

Best match rotations. In all experiments, a best match rotation analysis was used to quantify the orientation, reliability, and coherence of the hippocampal map. First, for the analysis of the rectangular and isosceles triangular chambers, rate maps were compressed to squares and equilateral triangles, respectively, by using anisotropic pixels when generating the rate maps (short dimension 1 cm x long dimension 1.5 cm pixels for the rectangle; short dimension 1 cm x long dimension 1.42 cm for the triangle). Next, for each pair of trials (66 comparisons for 12 trials), the rotation of the Trial A rate map (square/rectangle: 0º, 90º, 180º, or 270º; triangle: 0º, 120º, 240º) that maximized the similarity to the Trial B rate map for each cell was computed. Similarity was calculated as the pixel-to-pixel cross-correlation between the two rate maps. To measure the likelihood of observing each orientation, the percent of pairwise trial comparisons for which each rotation yielded the best match was calculated for each cell. These proportions were then averaged within each animal as the orientations of simultaneously-recorded cells are likely not independent.

Rate map similarity. To measure the similarity of rate maps across trials for each cell, the best match rotation correlation value was computed for each pair of trial comparisons, and then averaged across all pairwise trial comparisons. This yielded a single correlation value for each cell indicating the similarity of that cell's rate maps across trials after aligning all trials. To test significance, the average correlation value across all cells was computed and compared to a shuffled control. This shuffled control was generated by randomly shuffling the rate maps across cells and trials prior to quantifying the rate map similarity using the same method (1000 iterations). The average correlation value across cells was then compared to the average correlation values from 1000 iterations of this shuffled control.

Orientation coherence. To measure the orientation coherence of simultaneously-recorded cell pairs, the patterns of best match rotations across all pairwise trial comparisons for both cells was compared. The similarity between these best match rotation patterns was quantified as the proportion of pairwise trial comparisons for which the same rotation yielded the best match. Trial comparisons for which at least one cell in the pair was inactive were excluded. To assess the significance of this orientation coherence, pattern similarity was compared to a shuffled control created by shuffling the best match rotation pattern for each cell independently. A cell pair was considered significantly coherent if its similarity exceeded the 99th percentile of 1000 iterations of this shuffled control. Note that this measure is sensitive to the distribution of best match rotations. Since two orientations tend to occur more often in the rectangular chamber, chance correspondences between the shuffled best match rotations are relatively common. Thus it is more difficult to distinguish true coherence from chance in the rectangular chamber than in the square chamber, where the even distribution of best match rotations yields fewer accidental co-occurrences following shuffling. This measure is also sensitive to the location of place fields. Specifically, the orientations of cells with fields near the center of the chamber are less clearly determined, and thus the best match rotations of these cells are inherently more variable. Because of these sensitivities, this measure sets a lower bound on orientation coherence.

Average behavior rate maps. Average rate maps corresponding to two behaviors (correct and geometric error searches) were created for each cell by concatenating the position and spiking activity vectors across all included trials. These data were then treated as a single trial and used to construct rate maps as described above.

Predicting Behavior. Behavior was predicted on the basis of population activity using a leave-one-out procedure. First, average behavior rate maps were created from correct and geometric error trials as described above, excluding the to-be-predicted trial. Then, the withheld trial rate maps were compared to the average correct and average geometric error rate maps by correlating the population vectors. The predicted behavior for the withheld trial was then the behavior corresponding to the average map with the higher population vector correlation. To assess whether the hippocampal map predicted search behavior prior to that behavior, we used two methods. First, we predicted search behavior on each trial using the same average map method, but only including data from incrementally longer time intervals (0 s to 60 s, in 0.5s steps) starting from the beginning of the to-be-predicted trial. Second, we predicted search behavior on each trial using the same average map method, but only including data prior to the first search during that to-be-predicted trial.

Bayes Factor. Bayes Factors were computed to verify that the hippocampal map was oriented by geometry and not nongeometric features [S5, S6]. When testing for an influence of geometry on best match rotations in the rectangular chamber, we compared the alternative hypothesis that the map was oriented by geometry (i.e., $p(0^o) + p(180^o) > 0.50$) to the null hypothesis that the map was not oriented by geometry (i.e., $p(0^o) + p(180^o) = 0.50$). When testing for an influence of the nongeometric features on best match rotations in the rectangular chamber, we compared the alternative hypothesis that the map orientation was anchored by the feature (i.e., $p(0^o) > p(180^o)$) to the null hypothesis that the map orientation was insensitive to the feature (i.e., $p(0^o) = p(180^o)$). When testing for an influence of the nongeometric feature on best match rotations in the square chamber, we compared the alternative hypothesis that the map orientation was anchored by the feature (i.e., $p(0^o) > 0.25$) to the null hypothesis that the map orientation was insensitive to the feature (i.e., $p(0^o) = 0.25$). When testing for stability of best match rotations in the triangular chamber, we compared the alternative hypothesis that the map was oriented by geometry (i.e., $p(0^o) > 0.33$) to the null hypothesis that the map orientation was insensitive geometry (i.e., $p(0^o) = 0.33$). To compute summary Bayes Factors for each test, the corresponding Bayes Factor was computed for each cell separately, averaged within animal, and then combined across animals to yield the final cumulative Bayes Factor.

Behavior Coding

Behavior during the spatial reorientation task was coded by two experimenters prior to the analysis of any electrophysiological data. The search behavior for each trial was defined as the first location in which the mouse dug for the reward. A dig was defined as an instance in which the mouse used one or both front paws to remove bedding from the medicine cup. Only when bedding was visible outside of the cup was a dig categorized as such. While digging behavior was typically very apparent, there was disagreement between raters on a subset (7/70, 10%) of trials. A tiebreaking rater was used to resolve the disagreement in these cases.

Histology

Electrode placement was verified after the completion of the experiments by passing a current (0.1mA for 5sec) through the tetrodes that yielded unit data (52500 Lesion Making Device, Ugo Basile). Then, mice were perfused with 10% formalin solution (Fisher Scientific). The brains were removed and fixed at 4ºC for at least 24hrs in 10% formalin containing 3% potassium ferrocyanide (J.T. Baker) for Prussian blue staining. Next, the brains were transferred to a 30% sucrose solution and kept for at least 24hrs at 4ºC for cryoprotection. The tissue was cryosectioned (30μm thick, coronal) and Nissl stained using standard histological procedures [S7].

Supplemental References

1. Julian, J.B., Keinath, A.T., Muzzio, I.A., and Epstein, R.A. (2015). Place recognition and heading retrieval are mediated by dissociable cognitive systems in mice. Proc. Natl. Acad. Sci. *112*, 6503–6508.

2. Kentros, C.G., Agnihotri, N.T., Streater, S., Hawkins, R.D., and Kandel, E.R. (2004). Increased attention to spatial context increases both place field stability and spatial memory. Neuron *42*, 283–95.

3. Muzzio, I.A., Levita, L., Kulkarni, J., Monaco, J., Kentros, C., Stead, M., Abbott, L.F., and Kandel, E.R. (2009). Attention enhances the retrieval and stability of visuospatial and olfactory representations in the dorsal hippocampus. PLoS Biol. *7*, e1000140.

4. Ranck, J.B. (1973). Studies on single neurons in dorsal hippocampal formation and septum in unrestrained rats. I. Behavioral correlates and firing repertoires. Exp. Neurol. *41*, 461–531.

5. Gallistel, C.R. (2009). The importance of proving the null. Psychol. Rev. *116*, 439–453.

6. Jeffreys, H. (1998). The theory of probability (Oxford: Oxford University Press).

7. Powers, M.M., and Clark, G. (1955). An evaluation of cresyl echt violet acetate as a Nissl stain. Stain Technol. *30*, 83–8.